



Activated red mud loaded porcelain sand for the adsorption of As(V) from aqueous system

Shuwu Zhang^{a,b}, Xiaohui Wang^a, Bin Han^a, Wenchao An^c, Yuhuan Sun^a, Shihong Cui^a, Fayuan Wang^{a,*}

^aSchool of Environment and Safety Engineering, Qingdao University of Science and Technology, Shandong, Qingdao 266042, China, emails: wangfayuan@qust.edu.cn (F. Wang), 1043654689@qq.com (S. Zhang), 734147981@qq.com (X. Wang), 15005428505@163.com (B. Han), yhsun@qust.edu.cn (Y. Sun), 904279388@qq.com (S. Cui)

^bShandong Key Laboratory of Water Pollution Control and Resource Reuse, School of Environmental Science and Engineering, Shandong University, Qingdao, 266237, China

^cQingdao Environmental Monitoring Station, Shandong, Qingdao, 266003, China, email: 51275095@qq.com

Received 11 June 2019; Accepted 23 October 2019

ABSTRACT

An effective adsorbent for arsenate removal from aqueous system was synthesized by loading activated red mud on porcelain sand (ARPS). The loading was accomplished via chemical processes and thermal coating techniques. Several kinds of techniques which include scanning electron microscopy analysis, Brunauer–Emmett–Teller method were used to study the physic-chemical characteristics of the ARPS adsorbent. Adsorption of As(V) on the ARPS adsorbent was studied as a function of time, pH, and coexisting ion. The surface morphology of the ARPS was examined and the loading mechanisms were discussed in detail. Results from the batch experiments, conducted at an initial concentration of 0.2 ppm of arsenate, Langmuir and Freundlich isotherms equation were used to fit the adsorption isotherms. The adsorption kinetic curve for the As(V) fits well with the Langmuir adsorptive equation. The maximum equilibrium saturated adsorption capacity of ARPS on arsenate was 4.424 and 0.989 mg/g respectively at pH 6 and 9. Under acidic conditions, the adsorption rate of As(V) is higher, and the adsorption decreases obviously with the increase of pH. The leaching liquid by ARPS adsorbent after toxic characteristic leaching process test can reach the national standards of GB 5749-2006. So the ARPS adsorbent is safe when application. Accordingly, it is believed that the ARPS developed in this study is environmentally acceptable and industrially applicable to water treatment.

Keywords: Red mud; Activated red mud; Preparation; Adsorption; Arsenate

1. Introduction

Red mud is the fine-grained residue of alumina production from the Bayer process for extracting alumina from bauxite [1–5]. The application of red mud in environmental management and remediation has been investigated. It is widely available in large quantities and is expected to have a good affinity for arsenate, as it is rich in Fe and

Al oxides and hydroxides. The RM used in the study was obtained from Shandong Aluminum Corporation, China and the chemical composition (wt.%) is shown in Table 1. According to previous studies, modified red mud and activated red mud (ARM) are promising effective adsorptive materials for As(V) removal from water [6,7]. ARM has the highest adsorption capability and it has the highest surface area [8,9].

* Corresponding author.

Table 1
Composition and properties of RM (%)

Constituent	% (w/w)
SiO ₂	9.80
Al ₂ O ₃	10.4
Fe ₂ O ₃	25.02
MgO	1.70
CaO	10.08
Na ₂ O	4.80

The porcelain sand (PS) is widely used in water supply and sewage treatment as filter material [10]. The PS used in the study was obtained from JiangXi Filter Material Corporation, China. It has the following chemical composition (wt.%) listed in Table 2 and it shows that PS is primarily a mixture of Si and Al oxides. Therefore it has the potential for arsenate removal from aqueous system [11]. The single-point N₂ Brunauer–Emmett–Teller (BET) method indicated that the specific surface area of a typical PS sample was about 1.56 m²/g. In a preliminary study, the PS was directly used for arsenate removal from water [12], but the removal capability was low, hence it is not applicable in industrial waste-water treatment.

ARM is only available as fine powders and is difficult to be separated from aqueous solution after adsorption activity. United States Environmental Protection Agency has proposed iron oxide-coated sand filtration as an emerging technology for arsenate removal from small water facilities [13]. The problem of the solid–liquid separation for powder adsorbent can be resolved.

In this study, we attempted to load ARM on the surface of PS via chemical processes and high-temperature coating techniques. The loading of ARM on PS is supposed to be easily separated from aqueous systems. Furthermore, silica contained in the PS may perform as a binding agent which could increase the physical strength of the adsorbent [14]. Additionally, metallic elements such as silica initially contained in the PS could precipitate and coagulate with anionic arsenic ions, an ARM with high specific surface area and surface charge adsorb of arsenate, phosphorus, and other anions easily. The key point of the technique was the simultaneous generation of ARM and silica sol in-situ and eventually led to the formation of Fe–Si surface complexes which combined the iron oxide with the porcelain sand tightly.

Table 2
Composition and properties of PS used

Constituent	% (w/w)
SiO ₂	68–74
Al ₂ O ₃	14–20
Fe ₂ O ₃	<0.7
MgO	<0.7
CaO	0.5
Na ₂ O	0.4

2. Materials and methods

2.1. Materials

All glassware and sample bottles were soaked in diluted HCl solution for 24 h and washed three times with deionized water. All experiments were conducted in duplicate and the mean values were considered. Solutions were prepared from Na₂HAsO₄·7H₂O for As(V). A 1 g/L As(V) stock solution was prepared by dissolving 4.057 g Na₂HAsO₄·7H₂O in 1 L of distilled water. As(V)-bearing water was prepared by diluting As(V) stock solution to given As concentrations with deionized water. The pH of the solutions was adjusted with either HCl or NaOH solution.

2.2. Adsorbent preparation

The details of activated red mud on porcelain sand (ARPS) are as follows. First 300 g of PS is placed in a beaker, the raw RM was sieved and the particles below 177 μm were used for activation, 50 g of powder was added to 1 L of 1 M FeCl₃·6H₂O in a beaker containing PS, magnetically stirred for 1 h and aged for 24 h. Then 1 M NaOH solution was added dropwise to the mixture while stirring until the pH of the slurry was around 7.0. The slurry was continuously stirred by a magnetic stirrer for 2 h and aged for 24 h. The mixture was centrifuged and the obtained solid was washed with deionized water three times. The obtained solid was dried at 105°C. The diagram of ARPS adsorbent preparation is depicted in Fig. 1. The micro-graphs of ARPS and PS adsorbent are shown in Fig. 2.

PS is prepared with kaolin as the main raw material, filled with special conditioner, mixed evenly and prepared into PS with a rough surface, large specific surface area, high porosity, and hard appearance, to facilitate the load of ARPS adsorbent. The production process of PS is shown in Fig. 3.

The main methods of powder forming include compacting, extrusion molding and disc forming. The speed of the disc pelletizer used in this experiment is 20–30 r/min and the disc angle is 45°. The weight ratio of several raw materials was mixed evenly. Start the pelletizer and spray water by manual control. When the diameter of the pellet is about 0.5 mm, the machine was turned off. The pellets were taken out of the pelletizer and placed at room temperature for 24 h. They were roasted in a muffle furnace for 12 h.

In the granulation process, the temperature of calcination is the most important link. The PS strength is not enough and easy to become loose in the water when the temperature is low. The surface of PS is smooth and ARM is easy to fall off after loaded when the temperature is higher. The temperature of calcination was determined to be 800°C after the experiments. The prepared PS has a large specific surface area, surface roughness, and satisfies the requirement of the load. The influence of different temperatures of calcination on PS is shown in Table 3. The physical properties of the PS filter material prepared are shown in Table 4.

2.3. Analysis

All chemicals were of analytical grade and used without further purification. Arsenate was analyzed on the

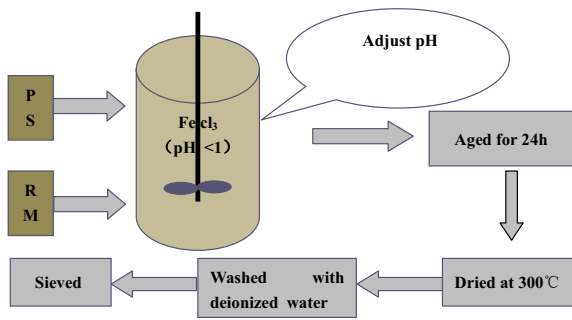


Fig. 1. Schematic diagram of ARPS adsorbent preparation.



Fig. 2. Micro-graphs of ARPS and PS adsorbent. Left: ARPS and Right: PS.

atomic fluorescence spectrometer (AF-610A) [15]. The specific surface area of the samples was determined by the BET nitrogen gas adsorption method using a Micromeritics ASAP2000V (Micromeritics, Norcross, GA) accelerated surface area and porosimetry [16]. The micro-graphs and micro-analysis of the samples were determined using a 30 kV HITACHI S-3000N (Hitachi, Tokyo, Japan) scanning electron microscopy (SEM).

2.4. Adsorption experiments

The batch adsorption experiments were conducted for the study of the adsorptive performance by the ARPS adsorbent. Adsorption studies were carried out by shaking $\text{Na}_2\text{HASO}_4 \cdot 7\text{H}_2\text{O}$ solution at 400 rpm in the bottles for 12 h at 20°C, and a background electrolyte of 0.01 M NaCl was used for all batch experiments. After equilibrium, the solutions were centrifuged at 5,000 rpm for 10 min and the supernatant was taken and analyzed for arsenate. Arsenate adsorbed was calculated as follows:

$$q = \frac{(C_0 - C_t)V}{m} \quad (1)$$

where q is the concentration of the arsenate adsorbed (mg/g), C_0 and C_t are the initial and final concentrations of

Table 3
Effect of different temperature on the character of PS

Calcination temperature	Porcelain sand performance
600°C	Low mechanical strength, easy to become scattered in water
800°C	The structure is compact, the surface has certain porosity, high mechanical strength, and suitable water absorption
1,000°C	High mechanical strength, smooth surface, not easy to load

Table 4
Physical characters of PS

Project	Indicators	Note
Compressive strength		<0.7
Resistance to temperature	>1,000°C	
Specific heat	628–837 J/kg, °C	
Specific gravity	2.3 g/cm ³	
Heap than quantity	1.9 g/cm ³	
Water absorption	5.2%–8.2%	
Percentage of damage	1.24%	

the arsenate in solution (mg/L), respectively. V is the solution volume (L) and m is the mass of adsorbent (g).

2.5. Leaching experiments

Referring to the standard leaching method notification No. 46 of the Ministry of Environment (Japan), the leaching amount of selected elements at different pH was examined. The solid/liquid ratio was 1:10, and the pH values of the extracting solvents were adjusted to 1–13, then vibrated for 6 h at 20°C and filtrated. Element concentrations in the filtrate were determined by inductively coupled plasma-atomic emission spectrometry [17,18].

3. Results and discussion

3.1. Characterizations of ARPS

3.1.1. Loading mechanisms and load capacity

The measurement results show that the surface areas of both PS and ARPS were about 1.56 and 10.1 m²/g. The surface area of ARPS increased by 70% compared to PS, because the ARPS adsorbent by loading on the surface of PS is larger than the surface area. The weight of ARM on the surface of PS was about 15.4 mg/g.

ARPS is a chemical reaction generated by activated SiO_2 and Al_2O_3 under the excitation of $\text{Ca}(\text{OH})_2$ to generate

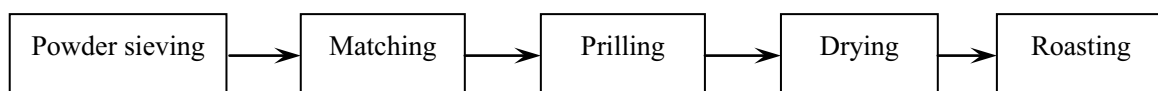
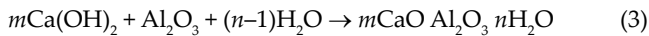
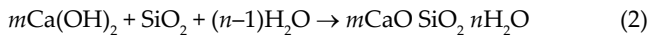


Fig. 3. Schematic diagram of PS preparation.

hydration products similar to Portland cement (calcium silicate hydrate and calcium aluminate hydrate), which is conducive to the loading of ARM adsorbent on the surface of PS. The chemical [19,20] equations are as follows:



The ARPS prepared are brown-red particles, which indicated that the ARPS adsorbent could be well loaded on the surface of PS. ARPS has a rougher surface and more pores than PS.

3.1.2. SEM and energy-dispersive X-ray spectroscopy analysis

SEM showed the effect of ARM on the PS surface erosion and collapse. The new surface area generated by acidification can be observed through the difference of SEM between PS and ARPS samples (Fig. 4). Moreover, it can also be seen from Fig. 4 that ARM particles are loaded on the PS particles perfectly and big-size composites are formed.

SEM and energy-dispersive X-ray spectroscopy (EDS) analysis results of arsenic adsorption by ARPS adsorbent are shown in Fig. 5. As can be seen from the figure, a little flocculent white precipitate was retained on the surface of the adsorbent, indicating that the adsorbed As(V) generated surface complex precipitate. The presence of As(V) was detected by energy spectrum analysis. The results of surface complexes are shown in Fig. 6.

3.2. Adsorption of arsenate to ARPS

3.2.1. Effect of pH value on adsorption

pH plays an important role in the adsorption of anions on metal oxides, and it is one of the important factors affecting the adsorption effect. The effect of pH value between 3 and 12 on ARPS adsorption of arsenate (initial arsenate concentration 1 mg/L, dosage 20 g/L, adsorption time 10 h) was investigated. The results are shown in Fig. 7.

The changing trend of ARPS affected by pH value was similar to that of ARPS adsorbent affected by pH value. As the pH of the solution increases, the positive charge on the surface of the ARPS gradually decreases, which reduces the electrostatic attraction of the ARPS to the anions in the water and reduces the removal rate. In addition, the increase in the pH of the solution reduces the hydrogen bond adhesion of the metal oxides on the ARPS surface, especially at the zero charge point pH or higher pH, the deprotonating of the metal oxide hydroxyl group makes the hydrogen bond adhesion weak.

3.2.2. Effect of different time on adsorption

The effect of ARPS adsorbent on the removal rate of As(V) ions (initial concentration of 1 and 2 mg/L) under different adsorption time conditions is shown in Fig. 8. The results showed that the adsorption of As(V) on ARPS adsorbent reached 40% within 3 min, and the adsorption increased with the increase of reaction time. As the adsorption approaches equilibrium, the adsorption quantity gradually approaches a limit value. Within 10 h, the adsorption of

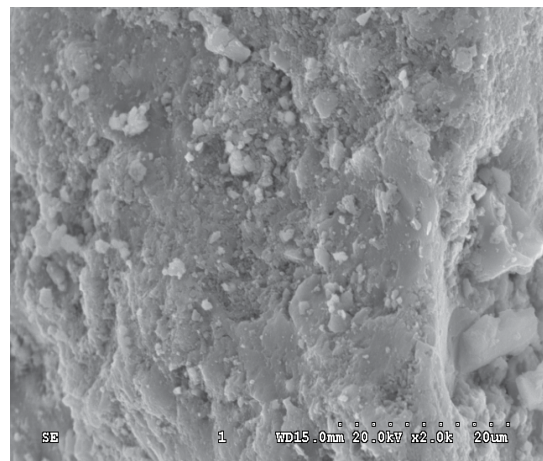


Fig. 5. SEM micro-graph of the ARPS adsorbent after adsorption of arsenate.

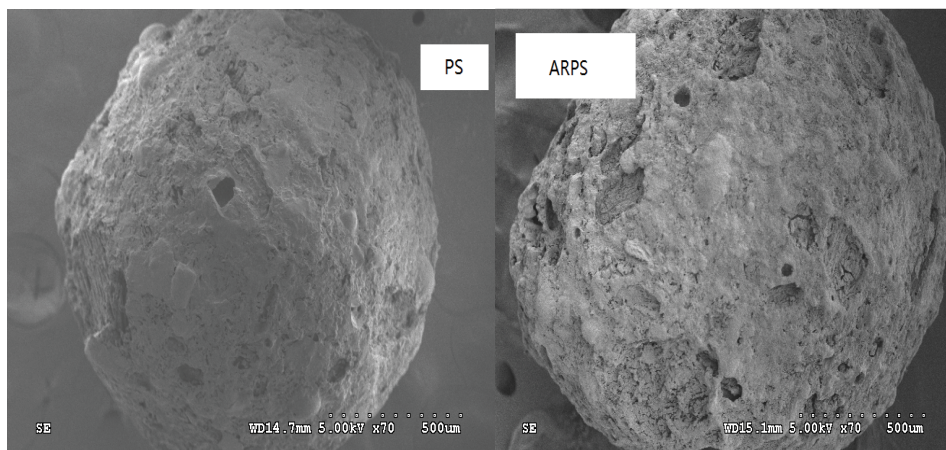


Fig. 4. SEM micro-graphs of the PS and ARPS.

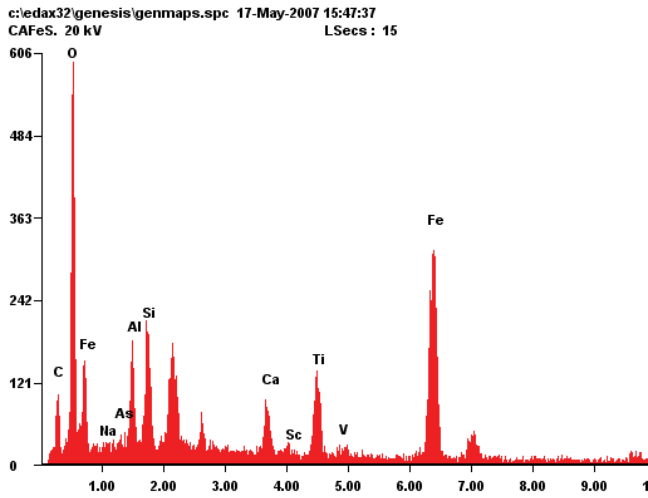


Fig. 6. EDS report of the ARPS adsorbent after adsorption of arsenate.

As(V) showed rapid adsorption and reached the maximum. After that, the adsorption tended to be balanced and stable, and the reaction time was prolonged. Studies have shown that the adsorption of As(V) on iron oxides includes two stages: the fast adsorption stage occurs before 5 min, and the slow adsorption stage occurs after 5 min. The adsorption efficiency of the slow stage was not determined by the concentration of As(V) in the solution, but it was determined by the adsorption amount of As(V) in the fast adsorption stage.

3.2.3. Adsorption isotherm

The saturation adsorption capacity of ARPS on arsenate was investigated. Arsenic solutions with different concentrations were prepared. 100 mL of solution was added to the 250 mL conical flask. The dosage of ARPS was 20 g/L to investigate the distribution of arsenate between solid and liquid phases at equilibrium. Langmuir and Freundlich adsorption isotherms were used to fit the experimental data. The results are shown in Fig. 9.

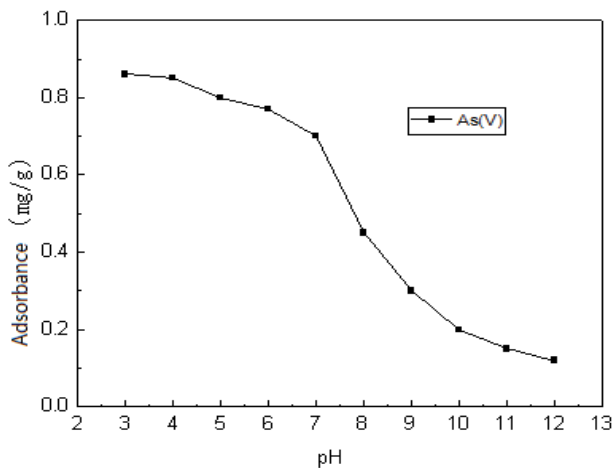


Fig. 7. Effects of pH on arsenate removal capacity.

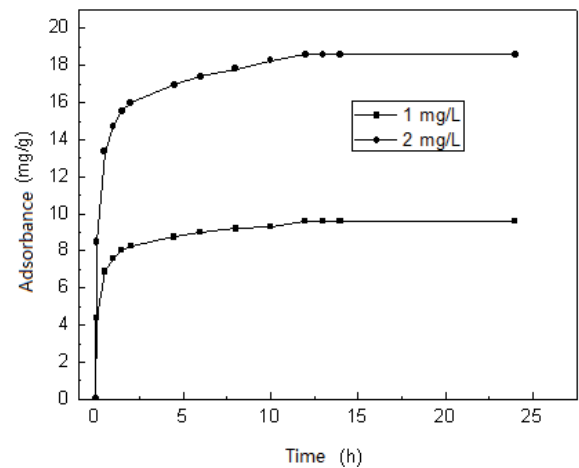


Fig. 8. Effects of time on arsenate removal capacity.

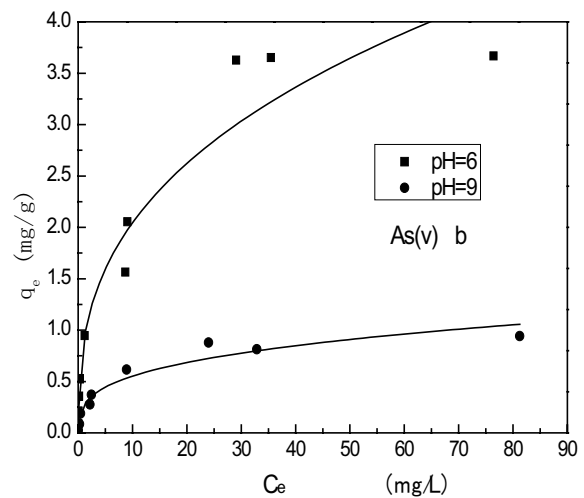
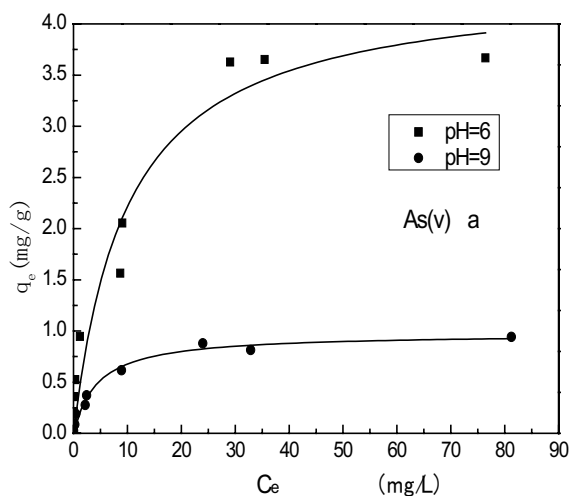


Fig. 9. Langmuir and Freundlich isotherm plots for arsenate and phosphate adsorption.

The fitting parameters of Langmuir equation and Freundlich equation are shown in Table 5. At pH6 and 9, the maximum equilibrium saturated adsorption capacity of ARPS on arsenate was 4.424 and 0.989 mg/g respectively.

3.2.4. Effect of solution ionic strength on the adsorption

The effect of ionic strength on the arsenate removal rate was investigated. It is a method to estimate the effect of ionic strength change on adsorption behavior. Hayes and they pointed out that the outer-sphere complex formed in the macroscopic performance is as follows: the adsorption tends to decrease with the increase of solution ionic strength; the formation of the inner-sphere complex showed that the adsorption did not depend on ionic strength, or the adsorption increased with the increase of ionic strength. This is due to the high activity of available nations in the solution, which can compensate for the surface of charge generated by the adsorption.

The effect of ionic strength on the adsorption removal rate of As(V) is shown in Fig. 10. The results showed that as the electrolyte concentration increased from 0.01 to 0.1 mol/L, the removal rate of As(V) remained unchanged. When the ionic strength in solution changes, the ions adsorbed by non-characteristic adsorption are more sensitive than adsorbed by characteristic adsorption because the electrolyte can form an outer-sphere complex through electrostatic interaction. The

results show that the main mechanism of action except for As(V) is characteristic adsorption, and As(V) forms an inner surface complex at the solid–liquid interface.

3.2.5. Discussion on adsorption mechanism

Studies have shown that the adsorption process of oxygen-containing anions is the surface complex reaction between anions, the surface of $\equiv \text{MOH}$, $\equiv \text{MOH}_2^+$ and other functional groups. Method was extended X-ray absorption fine structure (EXAFS) [21] from iron, the bond length of the coordination number reveals the As(V) is formed by force strong inner ring complexes, selective adsorption to the hydration or hydroxyl iron oxide. The surface of the complex model is the main mechanism of arsenate removal. The results of transmission Fourier transform infrared spectroscopy and attenuated total reflectance Fourier transform infrared spectroscopy showed that under the condition of high arsenic/iron ratio, arsenic radical and arsenate radical replaced two single surface of hydroxyl groups respectively and formed the binuclear binate complex Fe-O-AsO(OH)-O-Fe and Fe-O-As(OH)-O-Fe (2C) or nonnuclear binate complex (2E). In the case of a low As/Fe ratio, it is more conducive to the formation of mononuclear monodentate angular complex (1V).

The adsorption of As(V) by ARPS adsorbent can be regarded as the surface of complexation between the surface of the hydroxyl group and As(V) anion. The reaction of proton migration takes place on the surface of the hydroxyl group, which shows the amphoteric surface of characteristics and corresponds to charge changes. The proton migration equilibrium can have corresponding constants, namely the surface of coordination constant.

Table 5
Langmuir and Freundlich isotherm parameters for adsorption

pH	Langmuir equation			Freundlich equation		
	q_0 (mg/g)	b (L/mg)	R^2	k	n	R^2
As(V)						
6	4.424	0.1003	0.96	0.89386	2.78	0.94
9	0.989	0.2267	0.98	0.27066	3.22	0.93

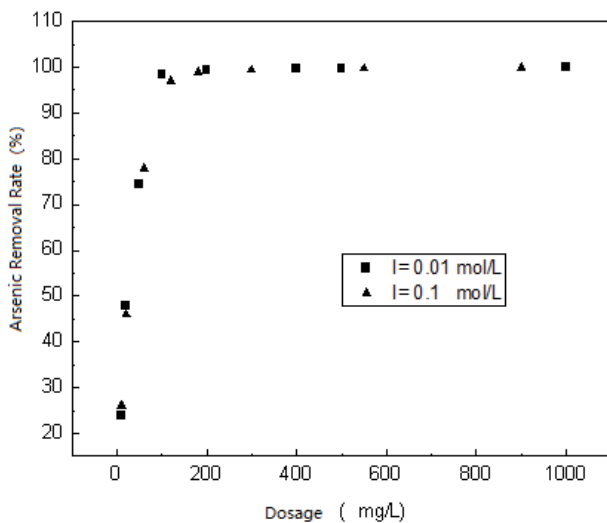
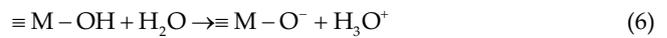
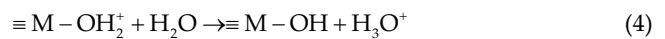
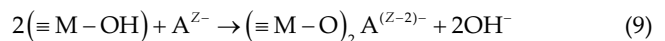
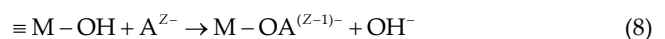


Fig. 10. Effect of the ionic strength on arsenate removal.

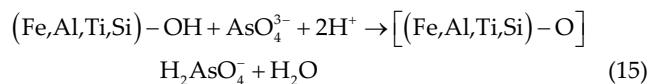
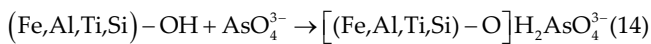
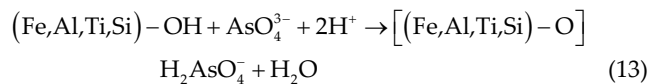
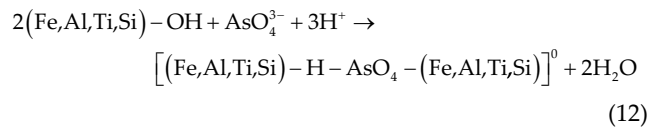
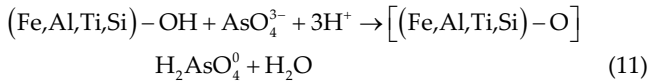
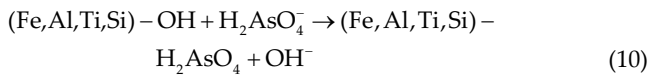


[] and { } respectively represent the combined concentration in the solution and the surface of combined concentration.

The surface of hydroxyl groups can form the surface of complexes with anions in aqueous solutions.



It can be seen that the complex equation of adsorption of As(V) by ARPS adsorbent is as follows:



3.3. Toxic characteristic leaching process

ARPS adsorbent was tested for the toxic characteristic leaching process (TCLP), an EPA invention commonly used to determine the potential for solid materials to release chemical toxins in a landfill environment. The leachate was analyzed and tested according to the GB5085.3-1996 method. The results are shown in Table 6. The results showed that the performance of the ARPS adsorbent TCLP test leaching solution completely reached the national GB 5749-2006 standard for drinking water.

Compared with RM, the TCLP test result of ARPS adsorbent is better, and RM is mainly the Al index slightly higher than the standard. The results show that the ARPS adsorbent has application safety.

4. Conclusions

- ARPS adsorbent was loaded on the surface of spherical PS filter material, and the spherical PS adsorption filter

material (ARPS) with ARM on the surface was successfully prepared. ARPS not only has the turbidity removal efficiency of ordinary ceramsite filter material but also has a strong adsorption ability for arsenic anions in water, which overcomes the problem that powder adsorbent is difficult to separate solid from liquid.

- The prepared ARPS adsorbent supported PS filter material (ARPS) has uniform particles and stable properties. The characterization of results showed that the external surface of ARPS was rough and porous. The specific surface area increased from 1.56 to 10.1 m²/g. The adsorption dose of ARM loaded on the surface of 1 g of PS was about 15.4 mg. The results of the strength test show that ARPS adhesion strength is high and meets the requirement of a fixed bed.
- The ionic strength in the solution had no effect on the adsorption and removal rate of As(V). The electrolyte concentration increased from 0.01 to 0.1 mol/L, and the removal rate of As(V) remained unchanged. The experimental results show that the main mechanism of action except for As(V) is characteristic adsorption. As(V) forms an inner-sphere surface complex at the solid-liquid interface.
- At pH 6 and 9, the maximum equilibrium saturated adsorption capacity of ARPS for arsenate was 4.424 and 0.989 mg/g respectively. The results show that ARPS adsorbents have good adsorption capacity for As(V) ions. The changing trend of ARPS affected by pH value was similar to that of ARPS adsorbent affected by pH value.
- The results of SEM adsorption of As(V) by ARPS adsorbent showed that a small amount of flocculated white precipitate remained on the surface of the adsorbent, indicating that the surface complex precipitate was produced after adsorption of As(V). EDS also detected the presence of As. The adsorption of arsenate by ARPS adsorbent belongs to the reaction mechanism of the surface of complex precipitation, and the adsorption process of oxygen-containing anions is the surface of complex reaction between anions, the surface of ≡ MOH, ≡ MOH₂⁺ and other functional groups.

Acknowledgments

The Key Technologies R&D Programme of China supported this work. The authors thank the Research Institute

Table 6
TCLP test results and comparison with China standards

	Fe (mg/L)	Al (mg/L)	Ti (mg/L)	Cr (mg/L)	Cu (mg/L)	Cd (mg/L)
ARM	0.009	0.012	0.004	0.006	0.0025	0.003
ARPS adsorbent	0.006	0.0085	0.001	0.002	0.00125	0.003
Standard request	0.3	0.2		0.05	1.0	0.005
	Mn (mg/L)	Hg (mg/L)	Pb (mg/L)	Ca (mg/L)	Mg (mg/L)	Zn (mg/L)
ARM	0.009	<0.001	0.001	0.62	0.025	0.03
ARPS adsorbent	0.003	<0.001	0.0006	0.0025	0.001	0.01
Standard request	0.1	0.001	0.01	450		1.0

of Shandong Aluminium for providing the raw red mud and support by Shandong Key Laboratory of Water Pollution Control and Resource Reuse (Grant No.2019KF15).

References

- [1] N. Ye, J. Yang, S. Liang, Y. Hu, J. Hu, B. Xiao, Q. Huang, Synthesis and strength optimization of one-part geopolymer based on red mud, *Constr. Build. Mater.*, 111 (2016) 317–325.
- [2] S.-P. Kang, S.-J. Kwon, Effects of red mud and alkali-activated slag cement on efflorescence in cement mortar, *Constr. Build. Mater.*, 133 (2017) 459–467.
- [3] X.B. Min, Y. Li, Y. Ke, M.Q. Shi, L.Y. Chai, K. Xue, Fe-Fe₂S₂ adsorbent prepared with iron powder and pyrite by facile ball milling and its application for arsenic removal, *Water Sci. Technol.*, 76 (2017) 192–200.
- [4] M. Ebrahiminejad, R. Karimzadeh, Hydrocracking and hydro-desulfurization of diesel over zeolite beta-containing NiMo supported on activated red mud, *Adv. Powder Technol.*, 30 (2019) 1450–1461.
- [5] S. Liu, J. Zeng, Application of thermally activated red mud in surface treatment of 5005 aluminum alloy, *Progr. Org. Coat.*, 133 (2019) 276–288.
- [6] R. Clemente, E. Arco-Lázaro, T. Pardo, I. Martín, A. Sánchez-Guerrero, F. Sevilla, M.P. Bernal, Combination of soil organic and inorganic amendments helps plants overcome trace element induced oxidative stress and allows phytostabilisation, *Chemosphere*, 223 (2019) 223–231.
- [7] L. Pietrelli, N.M. Ippolito, S. Ferro, V.G. Dovi, M. Vocciante, Removal of Mn and As from drinking water by red mud and pyrolusite, *J. Environ. Manage.*, 237 (2019) 526–533.
- [8] S. Aydin, M.E. Aydin, F. Beduk, A. Ulvi, Removal of antibiotics from aqueous solution by using magnetic Fe₃O₄/red mud-nanoparticles, *Sci. Total Environ.*, 670 (2019) 539–546.
- [9] B. Sızirici, I. Yildiz, Adsorption capacity of iron oxide-coated gravel for landfill leachate: simultaneous study, *Int. J. Environ. Sci. Technol.*, 14 (2016) 1027–1036.
- [10] B. Deng, G. Li, J. Luo, Q. Ye, M. Liu, M. Rao, T. Jiang, L. Bauman, B. Zhao, Selectively leaching the iron-removed bauxite residues with phosphoric acid for enrichment of rare earth elements, *Sep. Purif. Technol.*, 227 (2019) 115714.
- [11] G. Garau, A. Porceddu, M. Sanna, M. Silveti, P. Castaldi, Municipal solid wastes as a resource for environmental recovery: impact of water treatment residuals and compost on the microbial and biochemical features of As and trace metal-polluted soils, *Ecotoxicol. Environ. Saf.*, 174 (2019) 445–454.
- [12] S.W. Lin, K.A. Corrales-López, S. Perez-Sicairos, R.M. Félix-Navarro, Preparation, characterization and application of PS/SPEES-PES UF membranes for removal of ppm Cd²⁺ from aqueous media, *Polym. Bull.*, 74 (2017) 4729–4743.
- [13] Y.J. Liang, X.B. Min, L.Y. Chai, M. Wang, W.J. Liyang, Q. Pan, M. Okido, Stabilization of arsenic sludge with mechanochemically modified zero valent iron, *Chemosphere*, 168 (2017) 1142–1151.
- [14] S. Lata, S.R. Samadder, Removal of arsenate from water using nano adsorbents and challenges: a review, *J. Environ. Manage.*, 166 (2016) 387–406.
- [15] A. Kounina, M. Margni, A.D. Henderson, O. Jolliet, Global spatial analysis of toxic emissions to freshwater: operationalization for LCA, *Int. J. Life Cycle Assess.*, 24 (2018) 501–517.
- [16] H. Shahbeig, N. Bagheri, S.A. Ghorbanian, A. Hallajisani, S. Poorkarimi, A new adsorption isotherm model of aqueous solutions on granular activated carbon, *World J. Model. Simul.*, 9 (2013) 243–254.
- [17] D.-G. Liu, Y. Ke, X.-B. Min, Y.-J. Liang, Z.-B. Wang, Y.-C. Li, J.-C. Fei, L.-W. Yao, H. Xu, G.-H. Jiang, Cotreatment of MSWI fly ash and granulated lead smelting slag using a geopolymer system, *Int. J. Environ. Res. Public Health*, 16 (2019) 156.
- [18] K. Nguyen, B. Nguyen, H. Nguyen, H. Nguyen, Adsorption of arsenate and heavy metals from solutions by unmodified iron-ore sludge, *Appl. Sci.*, 9 (2019) 619.
- [19] G. Young, M. Yang, Preparation and characterization of Portland cement clinker from iron ore tailings, *Constr. Build. Mater.*, 197 (2019) 152–156.
- [20] K.L. Lin, B.Y. Chen, C.S. Chiou, C. An, Waste brick's potential for use as a pozzolan in blended Portland cement, *Waste Manage. Res.*, 28 (2010) 647–652.
- [21] L. Fang, Q. Shi, J. Nguyen, B. Wu, Z. Wang, I.M.C. Lo, Removal mechanisms of phosphate by lanthanum hydroxide nanorods: investigations using EXAFS, ATR-FTIR, DFT, and surface complexation modeling approaches, *Environ. Sci. Technol.*, 51 (2017) 12377–12384.